Polymers in Random Porous Materials: Structure, Thermodynamics, and Concentration Effects

Aidan P. Thompson[†] and Eduardo D. Glandt*

Department of Chemical Engineering, University of Pennsylvania, Philadelphia, Pennsylvania 19104-6393

Received March 13, 1996[⊗]

ABSTRACT: The distribution of dissolved macromolecules between a bulk solution and the interior of a porous substrate occurs in a variety of technologically important systems. The partition coefficient K, which is the ratio of concentration in the pores to that in the bulk, is primarily determined by the effective size of the polymer molecules. For dilute solutions, K decreases rapidly as the effective polymer dimensions exceed the average pore size. We have used liquid-state theory to construct a rigorous integral equation model for the structure of concentrated flexible linear polymers in the presence of a rigid matrix of discrete repulsive obstacles. We have used the structural information to calculate the thermodynamic properties of the polymer in these model porous materials. In particular, we have been able to calculate the partition coefficient as a function of concentration. The model provides good agreement with thermodynamic properties obtained from previous computer simulations of bulk polymer solutions as well as with our own simulations of polymers in porous materials.

I. Introduction

The equilibrium properties of molecular and polymeric fluids adsorbed within microporous disordered solids play an important role in a wide variety of technologies. The affinity of polymer molecules for the porous medium relative to the bulk fluid is a key factor in applications ranging from gel permeation chromatography to petroleum recovery. For this reason, the physical behavior of polymers in the presence of immobile obstacles has been a subject of considerable theoretical interest. Most experimental studies have focused on the partition coefficient. This is the relative concentration of polymer molecules in the pore fluid compared to that in the bulk. Measurements of partitioning of polystyrene[1] and dextran[2] solutions into porous glass indicate that K decreases with increasing molecular weight but increases with bulk concentration.

A similar increase of K with concentration has been observed in Monte Carlo simulations of polymers in simple pore geometries.[3,4] Bleha and co-workers[5] have observed a strong correlation between the rate of increase of K with concentration and the group A_2M_w, where A_2 is the second osmotic virial coefficient of the polymer in the solvent and M_w is the molecular weight. This led them to propose that the concentration effect is driven by deviations from ideality in the bulk solution. Teraoka *et al*. have constructed a thermodynamic model based on an approximate equation of state from renormalization group theory which predicts very strong concentration effects when the partition coefficient at infinite dilution is small.[6]

We have recently presented[7] calculations of structural properties of concentrated polymers in random porous materials using a microscopic statistical mechanical model originally proposed by Chandler.[8] This heuristic treatment incorporates the polymer RISM theory of Curro and Schweizer[9] with the treatment of fluids in quenched media developed by Madden and Glandt.[10,11] We have since developed a scheme[12] for calculating the thermodynamic properties of polymers from the structural information obtained from the integral equation model. In the next section we present the integral equation model. In section III we discuss the thermodynamic scheme which we have implemented. Comparison is made with the accurate molecular dynamics calculations of Gao and Weiner for the equation of state of the bulk polymer solutions.[13] Comparison is also made with our own Monte Carlo calculations for the activity of hard sphere chains in a bed of obstacles. In section IV we consider the effect of concentration on the partition coefficient, while in section V we compare the results of the model directly to the experimental measurements of the partition coefficient as a function of concentration.

II. Integral Equation Model

The integral equation model which we use is based on the Ornstein−Zernike equation for the structure of dense liquids. It was originally proposed by Chandler[8] and is described in more detail in our earlier paper.[7] The polymer molecules are viewed as flexible chains of spherical interaction sites, in accordance with Curro and Schweizer's[9] polymer version of the RISM model of Chandler and Andersen.[14] The porous material is introduced as a rigid matrix of randomly placed spherical obstacles. The polymer molecules interact with the obstacles but the obstacles are not affected by the polymer. In dealing with polymeric fluids, it is not feasible to treat each site on a chain individually. Instead, we make the usual assumption that for long chains most of the sites are very similar. Hence, we replace the individual site correlation functions by averages over all sites. This site-averaging approximation has been applied with considerable success by Curro and Schweizer.[9]

For the case of a single linear polymer component (p) with n identical sites per molecule and a porous material represented by only one type of interaction site, we can write the following pair of integral equations for the

[†] Present address: Union Camp Corp., Princeton, NJ 08543.
[⊗] Abstract published in *Advance ACS Abstracts,* May 1, 1996.

S0024-9297(95)00321-4 CCC: $12.00

polymer−polymer and polymer−matrix (site−site) correlations

$$h_{pm}(r) = \omega_p{*}c_{pm} + \omega_p{*}c_{pm}{*}\rho_m h_{mm} + \omega_p{*}c_{pp}{*}\rho_p h_{pm} \quad (1)$$

$$h_{pp}(r) = \omega_p{*}c_{pp}{*}\omega_p + \omega_p{*}c_{pm}{*}\rho_m h_{mp} + \omega_p{*}c_{pp}{*}\rho_p h_{pp} \quad (2)$$

where ρ_m and ρ_p are the number density of obstacles and polymer segments, respectively. The symbol * denotes a convolution integral.[15] The function $h_{mm}(r) = g_{mm}(r) - 1$ is the total correlation function for the matrix particles while $g_{mm}(r)$ is the corresponding pair correlation function. $h_{mm}(r)$ is the measure of the nonrandomness of the matrix and will be assumed to be known. Together, ρ_m and $h_{mm}(r)$ determine the physical characteristics of the material, such as porosity. Similarly, $h_{pm}(r)$ and $h_{pp}(r)$ are the polymer−matrix and *inter*molecular (or polymer−polymer) total correlation functions and are obtained by solving the above integral equations. $c_{pm}(r)$ and $c_{pp}(r)$ are the corresponding direct correlation functions, which act as propagators for the total correlation functions. The polymer correlations are best characterized by $g_{pp}(r) = h_{pp}(r) + 1$ and $g_{pm}(r) = h_{pm}(r) + 1$, the polymer−polymer and polymer−matrix site correlation functions, respectively. The correlation function $g_{pm}(r)$ is the relative density of polymer sites at a distance r from a matrix site. Similarly, $g_{pp}(r)$ is the relative density of polymer sites at a distance r from a polymer site, *not counting sites on the same molecule.* Correlations between sites on the same molecule are accounted for by the average *intra*molecular pair correlation function $\omega_p(r)$.

In order to solve the above equations, it is necessary to provide information about the polymer−polymer and polymer−matrix interactions. We wish to investigate the partitioning of polymers under good solvent conditions. Hence we represent the polymer molecules as chains of impenetrable hard spheres with effective diameter σ_p. The matrix sites are also assumed to be impenetrable to the polymer sites. The size of the obstacle hard spheres can be specified by the effective obstacle diameter σ_m or equivalently by the polymer−matrix collision diameter $\sigma_{pm} = (\sigma_p + \sigma_m)/2$. Continuous attractive interactions can be readily included in the model, but in our current calculations we only consider the entropic effects due to short-range repulsions between sites. We have solved the integral equations using the polymer RISM analog of the Percus−Yevick closure; for hard sphere interactions this produces the following closure constraints on the correlation functions:

$$g_{pm}(r) = 0, \qquad r < \sigma_{pm} \quad (3)$$

$$g_{pp}(r) = 0, \qquad r < \sigma_p \quad (4)$$

$$c_{pm}(r) = 0, \qquad r > \sigma_{pm} \quad (5)$$

$$c_{pp}(r) = 0, \qquad r > \sigma_p \quad (6)$$

As noted by Chandler,[8] these equations may be solved very efficiently using a variation of the scheme originally proposed by Chandler and Andersen.[14] The numerical procedure is described in detail in our earlier paper.[7]

One of the goals of this work is to propose a model for intramolecular interactions appropriate for the case of a polymer in a good solvent and in the presence of quenched obstacles. In our previous work[7] we used the freely jointed chain model (FJC) for the single-chain intramolecular pair correlation function $\hat{\omega}_p(k)$, which does not explicitly include any interactions between sites on the chain. A better description of the polymer would be that of a chain of mutually impenetrable hard spheres. While such a picture is still relatively simple, it is no longer possible to write down an exact expression for $\hat{\omega}_p(k)$. The reason, of course, is that in this model every site interacts with every other site on the molecule, no matter how far apart they are along the chain. One possible approach would be to calculate the true intramolecular structure in a self-consistent fashion. Another approach, which we will follow here, is to only include the effect of short-range interactions. This provides a good description of the *local* structure of the chain. The ommission of long-range and "solvent" interactions means that the scaling is still ideal. Although this approximation is known to be very good for polymer melts at high density, we expect it to yield incorrect scaling behavior in the present application, where the concentration of the polymer is low and obstacles are present.

A very general and elegant form of the short-range interaction model is the discrete Koyama semiflexible chain approximation (SCF) of Honnell, Curro, and Schweizer.[16] The discrete Koyama chain is composed of $n - 1$ linked rods of length l. The only correlations are between adjacent rods in the chain. The bond angle θ between each pair of adjacent rods is distributed on the range $(0,\pi)$ with a probability density $P_\theta(\theta)$. In the case of the freely jointed chain, $P_\theta^{FJC}(\theta) = \sin(\theta)/2$. In the case of a next-nearest-neighbor hard sphere repulsion, the lower bound on the bond angle θ_0 will be greater than zero. In their SFC model, Honnell *et al.*[17] control the chain stiffness by including an additional bending energy term, $E(1 + \cos\theta)$, where E is an effective stiffness parameter. The SFC probability density distribution for θ is then given by

$$P_\theta^{SFC}(\theta) = \frac{\sin(\theta)\exp(-E(1+\cos\theta))}{\int_{\theta_0}^{\pi}\sin(\theta)\exp(-E(1+\cos\theta))\,d\theta}; \qquad \cos\theta_0 = 1 - \left(\frac{\sigma_p^2}{2l^2}\right) \quad (7)$$

If the effective stiffness parameter is set to zero, one recovers what we refer to as the hard sphere chain model (HSC)

$$P_\theta^{HSC}(\theta) = \frac{\sin(\theta)}{(1+\cos\theta_0)}; \qquad \cos\theta_0 = 1 - \left(\frac{\sigma_p^2}{2l^2}\right) \quad (8)$$

The exact intramolecular distribution functions $\hat{\omega}_{\alpha\gamma}(k)$ for the HSC model and for the more general SFC model are not known. Instead, we will use the following approximate Koyama expression:

$$\hat{\omega}_{\alpha\gamma}(k) = \frac{\sin(kB_{\alpha\gamma})}{kB_{\alpha\gamma}} e^{-k^2 A_{\alpha\gamma}^2} \quad (9)$$

This is the product of two structure factors, the first is for a rigid rod of length $B_{\alpha\gamma}$, and the second is for a Gaussian spring with mean square extension $6A_{\alpha\gamma}^2$. The appropriate choices for $B_{\alpha\gamma}$ and $A_{\alpha\gamma}$ may be obtained[16] by equating the Koyama and SFC analytical expressions for $\langle r_{\alpha\gamma}^2\rangle$ and $\langle r_{\alpha\gamma}^4\rangle$.

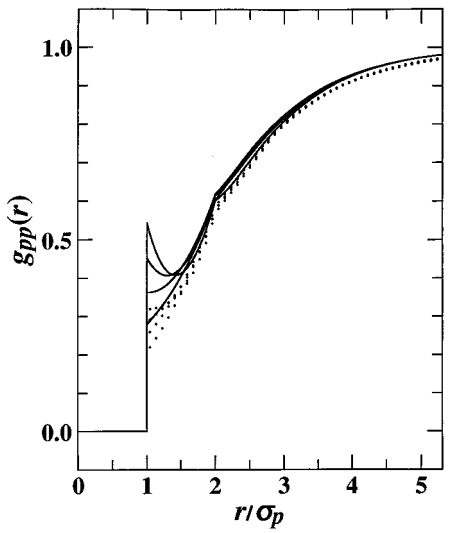

Figure 1. Comparison of the integral equation model (solid lines) with Monte Carlo simulations (points) for $g_{pp}(r)$. The results are for 20-segment hard sphere chains at a volume fraction $\eta_p = 0.1$ in a matrix of randomly placed spheres. The curves correspond to porosities $\epsilon = 0.285$, 0.433, 0.658, and 0.959, in order of decreasing contact value.

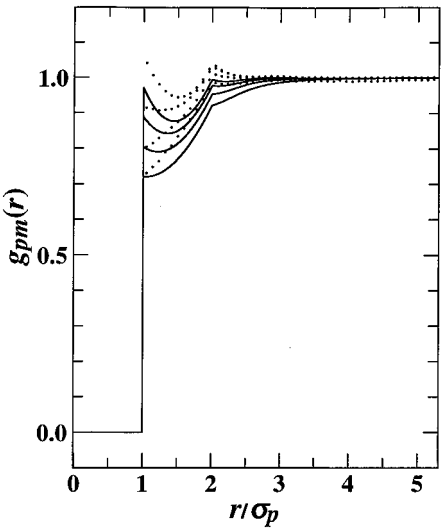

Figure 2. Comparison of the integral equation model (solid lines) with Monte Carlo simulations (points) for $g_{pm}(r)$. The results are for 20-segment hard sphere chains at a volume fraction $\eta_p = 0.1$ in a matrix of randomly placed spheres. The curves correspond to porosities $\epsilon = 0.285$, 0.433, 0.658, and 0.959, in order of decreasing contact value.

The above approach to the excluded volume problem, while approximate, provides an accurate description of the short-range structure of the polymer molecules. The neglect of long-range repulsions results in the underestimation of the true size of hard sphere chains. Long-range overlap also trends to lower the effective volume occupied by the polymer. To correct for this, the effective polymer volume fraction can be defined by $\eta_p = (1 - \Delta_n)\rho_p\sigma_p{}^3\pi/6$, where Δ_n is the average fractional overlap volume of the semiflexible chain. Honnell *et al.*[16] approximated Δ_n using the average sum of pairwise overlap volumes

$$\Delta_n = \frac{1}{n}\int_0^{\sigma_p}\left(1 - \frac{3r}{2\sigma_p} + \frac{r^3}{2\sigma_p{}^3}\right)\left(\sum_{\alpha,\gamma>\gamma}\omega_{\alpha\gamma}(r)\right)4\pi r^2\,dr \qquad (10)$$

When used to model bulk polymer solutions, the HSC model has been found to achieve reasonably good agreement with pair correlation functions obtained by Monte Carlo simulation of "true" hard sphere chains. We have tested the performance of the HSC model for polymers in porous materials. We modeled the porous matrix as a sintered bed of randomly centered spheres, for which $h_{mm}(r) = 1$. The polymer chains were made up of tangential hard spheres of the same size as the obstacles, so that $l = \sigma_p = \sigma_m$. The porosity ϵ was defined as the free volume fraction available to the center of one polymer segment and is given by the following exact expression:

$$\epsilon = \exp\left[-\frac{4\pi}{3}\sigma_{pm}{}^3\rho_m\right] \qquad (11)$$

where $\sigma_{pm} = (\sigma_p + \sigma_m)/2$ as before. A comparison was made with Monte Carlo results for 75 molecules of hard sphere 20-mers simulated in the presence of 10 different configurations of randomly placed hard sphere obstacles. The number of obstacles and the size of the simulation cell were varied to achieve the desired porosity and polymer volume fraction. In Figure 1 the polymer–polymer pair correlation function is shown for porosities $\epsilon = 0.285$, 0.433, 0.658, and 0.959, listed here in descending order of $g_{pp}(r)$ at contact. The polymer volume fraction is $\eta_p = 0.1$. It can be seen that $g_{pp}(r)$ is sensitive to porosity only at very short separations. The correlation hole persists, even at the lowest porosity. The theory tends to overestimate the contact value of $g_{pp}(r)$ somewhat and also overestimates the sensitivity to porosity. In Figure 2 the corresponding results for $g_{pm}(r)$ are shown. Here we see a greater sensitivity to porosity. The theory in this case appears to underpredict the simulation results somewhat in this case. The figures indicate that the overall performance of the theory is better than in the case of the polymers without intramolecular excluded volume. This difference can be attributed to the fact that the HSC model provides a good description of bulk hard sphere chains. Moreover, the hard sphere chain intramolecular structure is insensitive to the presence of the porous material.

III. Calculation of Thermodynamic Properties

The integral equation model allows the calculation of average structural properties of the polymer, such as the polymer–polymer and polymer–matrix pair correlation functions. This information is of limited practical use on its own; generally, thermodynamic properties are of greater interest. The most useful of these is the polymer chemical potential, which is necessary to calculate the partition coefficient K. For monomeric fluids, the pressure, energy, and compressibility equations[15] provide exact and mutually consistent routes to the thermodynamics. However, when approximations such as that of Percus and Yevick are introduced, consistency among these approaches is lost, and agreement with simulations may be poor, particularly at low temperatures.[17]

For molecular fluids, composed of multiple interaction sites, the situation becomes more complex. Although integral equations such as RISM yield spherically symmetric site–site pair correlation functions, the thermodynamic relations involve the more complex molecule–molecule pair correlation function. Lowden and Chandler[18] succeeded in rewriting the compressibility equation in terms of the RISM site–site pair

correlation function for hard sphere diatomics. The resultant equation of state underpredicted the pressure, particularly at higher densities. They obtained better results using a charging method for the Helmholtz free energy, similar to the one we use below.

Curro and Schweizer extended the RISM model for hard sphere diatomics to a hard sphere chain model in their work on polymer RISM.[19] Although they were primarily interested in modeling polymer melts, McMillan−Mayer theory[20] allows us to use the same model to describe polymer solutions. In this approach, a formal equivalence is established between the absolute pressure of a one-component fluid and the osmotic pressure of the solution. Thus, Curro and Schweizer's exact extension of the compressibility equation to polymer RISM model can be invoked for polymer solutions

$$\frac{\beta\Pi}{\rho_p} = \frac{1}{\rho_p}\int_0^{\rho_p}[\hat{\omega}_p(0) + \rho'_p\hat{h}_{pp}(0)]^{-1}\,d\rho'_p \qquad (12)$$

where Π is the osmotic pressure and $\beta = (kT)^{-1}$, k is Boltzmann's constant, and T is the temperature. In eq 12 ρ_p is the polymer concentration in segments per unit volume. The quantity in square brackets is the full polymer structure factor; the intramolecular structure factor $\hat{\omega}_p(k)$ must be specified *a priori*. The intermolecular contribution $\rho_p\hat{h}_{pp}(k)$ is obtained from the polymer RISM integral equations. Curro and Schweizer[19,21] also developed an approximation to the pressure equation for flexible molecules. Since the exact form of the pressure equation involves three-body correlations, whereas RISM theory only yields pair correlations, they used a simple superposition approximation. For hard sphere polymers, the approximation yields[22]

$$\frac{\beta\Pi}{\rho_p} = \frac{1}{n} + \frac{2\pi}{3}g_{pp}(\sigma_p)\left[1 + \frac{1}{n\pi^2}\int_0^\infty(\sin K - K\cos K)\rho_p\hat{h}_{pp}(k)\frac{\partial\omega_p}{\partial K}\,dK\right] \qquad (13)$$

where K is the dimensionless wavenumber $k\sigma_p$. The contact value of the intermolecular site−site pair correlation function $g_{pp}(\sigma_p)$ must also be obtained from the polymer RISM equations.

There is another route to the thermodynamics which has not been used extensively in the past. It describes in mathematical form the process of introducing an additional polymer molecule (the so-called "solute") by expressing its partial interaction ϕ_s as a continuous function of a coupling parameter ξ. The following boundary conditions must be met

$$\phi_s(\{\mathbf{R}^{N+1}\};\xi{=}0) = 0 \qquad (14)$$

$$\phi_s(\{\mathbf{R}^{N+1}\};\xi{=}1) = \phi_{N+1}(\{\mathbf{R}^{N+1}\}) \qquad (15)$$

where ϕ_{N+1} is the full interaction of a molecule with the rest of the system. The chemical potential of the polymer may be formally written as $\mu = \mu^0 + kT\ln\gamma$, where μ^0 is the chemical potential of noninteracting polymer molecules at the same temperature and density and γ is the polymer activity coefficient. $kT\ln\gamma$ is simply the residual free energy, that required to insert the additional molecule, which can be expressed[17] as an integral over ξ

$$kT\ln\gamma = \int_0^1\left\langle\frac{\partial\phi_{N+1}(\{\mathbf{R}^{N+1};\xi\})}{\partial\xi}\right\rangle_\xi d\xi \qquad (16)$$

where the subscript ξ indicates that the average is obtained using the $N + 1$ particle canonical ensemble at the value of the coupling parameter.

For systems with hard sphere interactions, it is convenient to let the solute collision diameter vary linearly with the coupling parameter. This process is the key concept underlying scaled particle theory.[23] It is also related to the "charging potential method" of Lowden and Chandler.[18] As the additional molecule is added to the polymer−matrix model described above, each of its segments presents collision diameters of σ_{sm} and σ_{sp} to the matrix particles and to the polymer segments, respectively. This scaling leads to the following equation for the activity coefficient

$$\ln\gamma = n\rho_m\int_0^{\sigma_{pm}}4\pi\sigma_{sm}^2G_{sm}(\sigma_{sm})\,d\sigma_{sm} + n\rho_p\int_0^{\sigma_p}4\pi\sigma_{sp}^2G_{sp}(\sigma_{sp})\,d\sigma_{sp} \qquad (17)$$

where σ_{sm} and σ_{sp} are the instantaneous contact separations for the solute−matrix and solute−polymer hard sphere interactions. $G_{sm}(\sigma_{sm})$ and $G_{sp}(\sigma_{sp})$ are the contact values of the solute−matrix and solute−polymer pair correlation functions. This type of equation has been found to give good results for the monomeric fluid−matrix model.[12,24] Since in the current work the solute is a polymer of n segments, the solute−matrix and solute−polymer pair correlation functions are given by the following equations:

$$h_{sm}(r) = \omega_s{*}c_{sm} + \omega_s{*}c_{sm}{*}\rho_m h_{mm} + \omega_s{*}c_{sp}{*}\rho_p h_{pm} \qquad (18)$$

$$h_{sp}(r) = \omega_s{*}c_{sp}{*}\omega_p + \omega_s{*}c_{sm}{*}\rho_m h_{mp} + \omega_s{*}c_{sp}{*}\rho_p h_{pp} \qquad (19)$$

These equations can be solved in a manner similar to that used for eqs 1 and 2. However, since $\rho_s = 0$, the correlations h_{sm} and h_{sp} do not appear on the right-hand side of the integral equations, which become linear and can thus be efficiently solved using standard matrix techniques. $G_{sm}(\sigma_{sm})$ and $G_{sp}(\sigma_{sp})$ are fairly smooth functions of the collision diameters and so only nine equally spaced interior points (in addition to the two limits of integration) were used to evaluate the integrals in eq 17. Since the self-interaction does not vary, we have approximated ω_s by ω_p.

We have this method to model the bulk polymer simulations of Gao and Weiner.[13] In order to compute the pressure from the activity coefficient, we have used the following equation, which can be derived from the Gibbs−Duhem relation.[25]

$$\frac{n\beta\Pi}{\rho_p} = 1 + \ln\gamma - \frac{1}{\rho_p}\int_0^{\rho'_p}\ln\gamma\,d\rho'_p \qquad (20)$$

The results of the scaled polymer method are compared with the previous equations of state in Figure 3−5. The scaled polymer approach is very accurate for the 16-segment polymers. For the longer polymers, it underpredicts the simulation values somewhat, but it is much more accurate than either the compressibility or the pressure equations of state. The success of the scaled

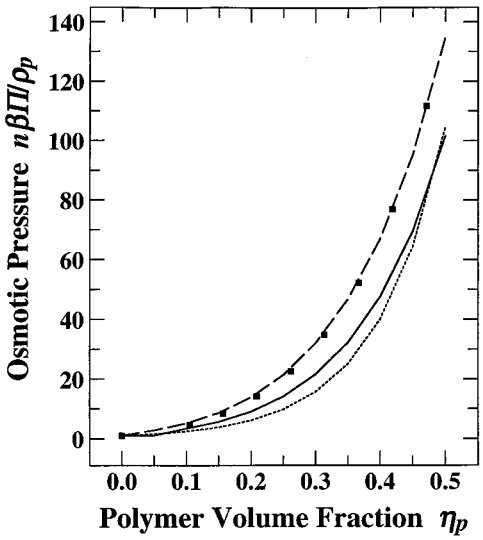

Figure 3. Osmotic pressure versus polymer volume fraction for linear polymers composed of 16 tangential hard spheres. The black squares are the simulation results of Gao and Weiner.[12] The long-dashed curve was obtained from the polymer RISM scaled polymer equation. The dashed and solid curves were calculated from the polymer RISM compressibility and pressure equations, respectively.

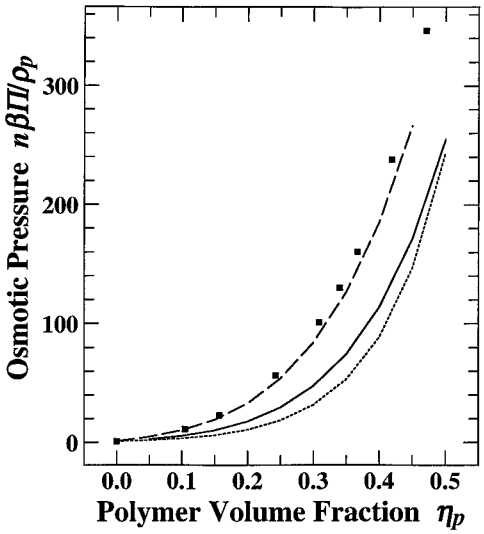

Figure 4. Osmotic pressure versus polymer volume fraction for linear polymers composed of 51 tangential hard spheres. The black squares are the simulation results of Gao and Weiner.[12] The long-dashed curve was obtained from the polymer RISM scaled polymer equation. The dashed and solid curves were calculated from the polymer RISM compressibility and pressure equations, respectively.

polymer method can be attributed to the fact that, unlike the compressibility route, it depends only on the short-range structure of the fluid, which is accurately modeled by polymer RISM theory. The same is true of the pressure equation, but this method involves a superposition approximation for the three-body term.

In order to test the accuracy of the method for polymers in porous materials, we have performed our own Monte Carlo simulations of hard sphere chains in a packed bed of nonoverlapping obstacle spheres to calculate the partition coefficient at infinite dilution as a function of porosity. The condition of partitioning equilibrium is

$$\mu(\rho_p) = \mu^b(\rho_p^b) \tag{21}$$

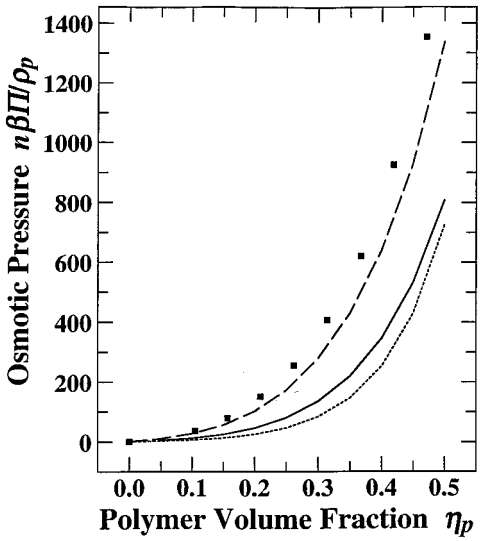

Figure 5. Osmotic pressure versus polymer volume fraction for linear polymers composed of 201 tangential hard spheres. The black squares are the simulation results of Gao and Weiner.[12] The long-dashed curve was obtained from the polymer RISM scaled polymer equation. The dashed and solid curves were calculated from the polymer RISM compressibility and pressure equations, respectively.

where $\mu = \mu^0 + kT \ln \gamma$. Combining eq 21 and the ideal-gas law leads to

$$K(\rho_p^b) = \frac{\rho_p}{\rho_p^b} = \frac{\gamma^b(\rho_p^b)}{\gamma(\rho_p)} \tag{22}$$

In general, eq 22 cannot be solved directly for K for a given value of ρ_p^b. Instead eq 21 must first be solved for ρ_p. In the limit where ρ_p^b goes to zero, however, eq 22 simplifies to

$$K_0 = \frac{\gamma_0^b}{\gamma_0} \tag{23}$$

where the subscript zero indicates infinite dilution. The activity coefficient γ has been defined in a manner which does not include the intramolecular contribution to the partition function; thus $\gamma_0^b \equiv 1$. In the case of the Monte Carlo simulations, the intramolecular contributions cancel out when the ratio is taken. For hard sphere interactions, K_0 is the probability that a randomly generated self-avoiding polymer does not overlap with any of the matrix obstacles.

To calculate γ_0 for each porosity, ten realizations of 32 000 nonoverlapping obstacle spheres of diameter σ_m were generated. The biased insertion method of Frenkel *et al.*[26] was used to compute the activity coefficient of hard sphere chains in the matrix and in the bulk with bond length $l = \sigma_p = \sigma_m$. In the integral equation theory, we once again used the HSC model for the intramolecular distribution function. A nonoverlapping hard sphere model was used for the matrix structure. The nearly exact results of the Monte Carlo simulations and the approximate results for the integral equation theory using the scaled polymer equation are compared in Figure 6. The theory predicts the simulation results very accurately.

The strong dependence of the partition coefficient on porosity ϵ takes the form of a polymer law $K_0 \sim \epsilon^n$. This is due to the fact that the insertion of one polymer

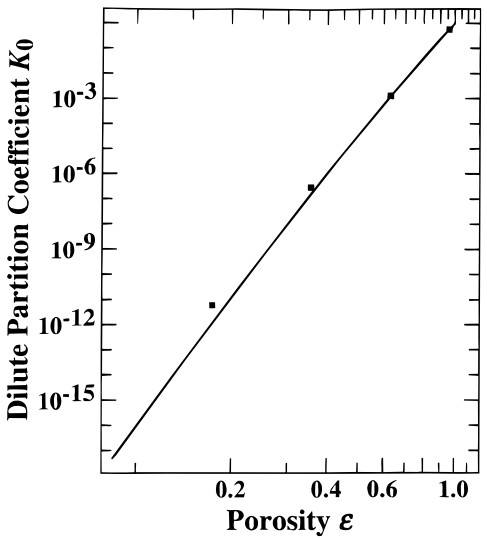

Figure 6. Partition coefficient at infinite dilution K_0 versus porosity ϵ for a 20-segment hard sphere chain in a matrix of nonoverlapping obstacles. The points were obtained by Monte Carlo simulation, and the line was obtained from the scaled polymer equation.

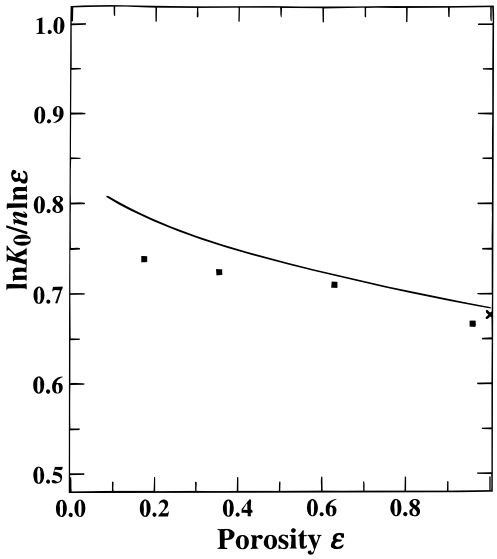

Figure 7. Plot of $\ln K_0/(n \ln \epsilon)$ versus porosity ϵ for a 20-segment hard sphere chain in a matrix of nonoverlapping obstacles. The points were obtained by Monte Carlo simulation, and the line was obtained from the scaled polymer equation. The data point at $\epsilon = 1$ was estimated from eq 25.

molecule requires the insertion of n segments. If the segment locations were independent of each other, the overall insertion probability would be ϵ^n, by definition of the porosity. The correlations between the segments result in deviations from this value. In Figure 7 we factor out this dependence by plotting $\ln K_0/(n \ln \epsilon)$ versus ϵ. A weak residual dependence on ϵ can now be seen. The deviation of the theory from the simulation results is now more pronounced. The theory performs best at high porosities but appears to be quite accurate in all the cases studied. $\ln K_0/(n \ln \epsilon)$ is the excess free energy of insertion relative to that of inserting n uncorrelated segments. The relative excess free energy is always less than unity for reasonable porosities. This is due to the self-screening of the polymer−matrix interactions. This screening effect is greatest in the limit $\epsilon \rightarrow 1$, in which case the relative excess free energy is given by

$$\ln K_0/n \ln \epsilon = \frac{v_e(n)}{n v_e(1)}, \qquad \epsilon \rightarrow 1 \tag{24}$$

where $v_e(n)$ is the average volume excluded by a polymer of n segments to the center of one matrix particle. This excluded volume can be well approximated by the following equation due to Dickman and Hall:[25]

$$v_e(n) = v_e(3) + (n - 3)(v_e(3) - v_e(2)) \tag{25}$$

In the present case, where $n = 20$ and $\sigma_m = \sigma_p = l$, we obtain a limiting value for the excess free energy $v_e(n)/nv_e(1) = 0.6768$, which is included in Figure 7. This appears to be a slight overestimate, which should be expected, since eq 25 double counts the small regions where four excluded volume spheres overlap.

IV. Effect of Concentration on Polymer Partitioning

In the previous section, we demonstrated that the scaled polymer method provides a tractable and accurate method for estimating the chemical potential of polymers in the bulk and in random porous materials. In this section, we use the method to investigate the effect of concentration on the partition coefficient. When the bulk polymer concentration is nonzero, it is necessary to solve eq 21 for ρ_p. This is achieved by evaluating the quantities $\mu^b(\rho_p^b)$ and $\mu(\rho_p)$ for a range of discrete values of ρ_p^b and ρ_p using the scaled polymer method of eq 17. An interpolation scheme is then used to evaluate the inverse functions $\rho_p^b(\mu)$ and $\rho_p(\mu)$ at a series of discrete values of the argument μ. For each value of μ the partition coefficient is given by

$$K(\rho_p^b(\mu)) = \frac{\rho_p(\mu)}{\rho_p^b(\mu)} \tag{26}$$

In this manner it is possible to generate plots of K versus ρ_p^b efficiently.

In the following section, the use of the method to model a particular experimental system is discussed. First we consider the general dependence of K on porosity, molecular weight, and concentration. Once again, we employ the hard sphere chain model with a bond length $l = \sigma_p = \sigma_m$. The nonoverlapping hard sphere model is used for the matrix structure. The porosity is defined as the volume available to the center of one polymer segment. In the case where $\sigma_m = \sigma_p$, ϵ is accurately approximated by the Carnahan−Starling equation[27]

$$\epsilon = \exp\left[-\frac{\eta_m(8 - 9\eta_m + 3\eta_m^2)}{(1 - \eta_m)^3}\right] \tag{27}$$

where $\eta_m = \rho_m \sigma_m^3 \pi/6$ is the volume fraction occupied by the matrix. In Figures 8−10 we show results for three different model porous materials with porosities of $\epsilon =$ 0.922, 0.376, and 0.085, respectively. In each case a very strong increase of K with concentration is observed. This effect is greatest for the lowest porosity and the longest polymer. In Figure 11 the curves for $n = 20$ are shown on a log−log plot. It is apparent in this plot that although the value of K_0 decreases sharply with ϵ, the value of K at high concentrations is relatively insensitive to porosity. The characteristic S-shape

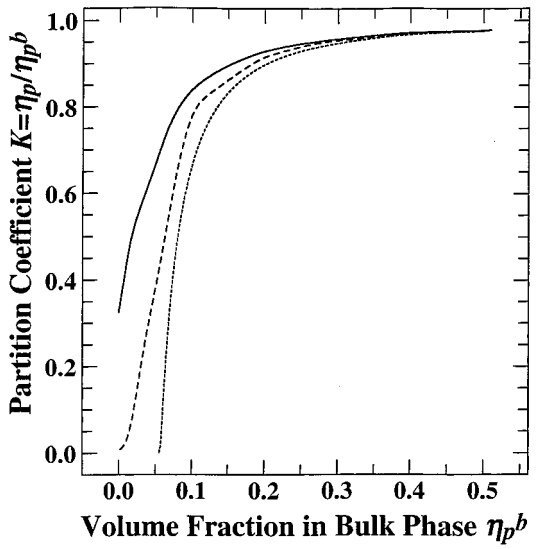

Figure 8. Partition coefficient K versus polymer volume fraction in the bulk for hard sphere polymers of 20, 100, and 2000 segments. The porous material is composed of nonoverlapping hard spheres with a porosity $\epsilon = 0.922$.

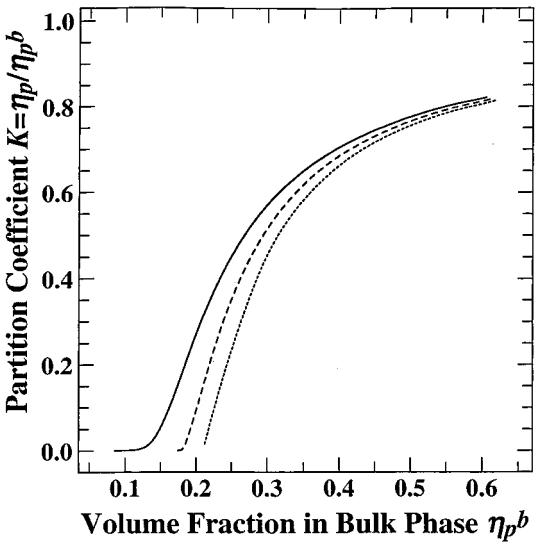

Figure 9. Partition coefficient K versus polymer volume fraction in the bulk for hard sphere polymers of 20, 100, and 2000 segments. The porous material is composed of nonoverlapping hard spheres with a porosity $\epsilon = 0.376$.

curves can be viewed as having three separate parts. In the first part, both the pore phase and the bulk phase are so dilute that they behave as ideal solutions, so that the activity coefficient γ is independent of concentration and the partition coefficient remains constant. In the second part, polymer−polymer interactions start to become important in the bulk phase and it becomes nonideal, causing the activity coefficient to increase. This causes K to increase strongly with concentration. Finally in the third part of the curve, the concentration in the pore phase rises to the point where it too becomes nonideal and so K begins to level off again.

This type of behavior has also been predicted recently by Karasz and co-workers[6] using a completely different thermodynamic model. Large changes in the measured diffusivity of polystyrene in controlled-pore glass which occur when the bulk concentration is increased may be caused by excatly this type of concentration effect. In both their model and ours, the increase in the partition coefficient K with polymer concentration is driven by

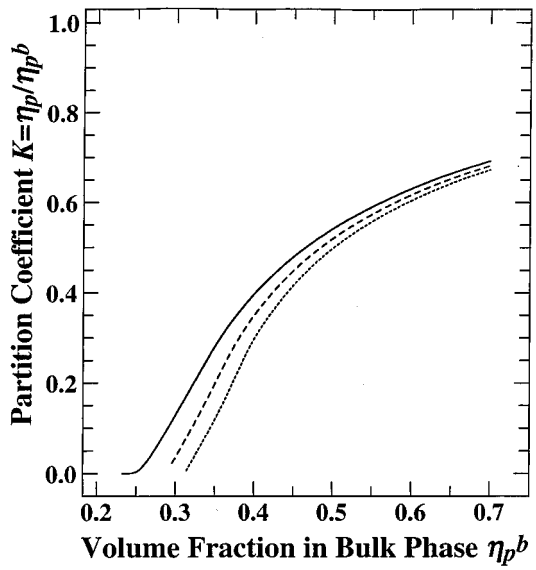

Figure 10. Partition coefficient K versus polymer volume fraction in the bulk for hard sphere polymers of 20, 100, and 2000 segments. The porous material is composed of nonoverlapping hard spheres with a porosity $\epsilon = 0.085$.

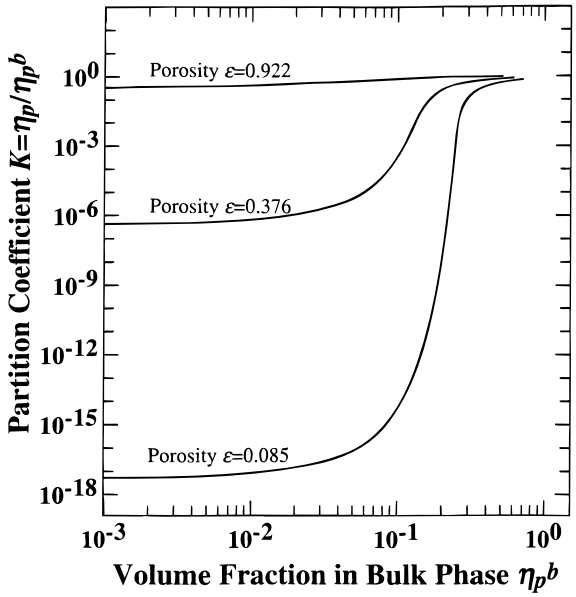

Figure 11. log−log plot of partition coefficient K versus polymer volume fraction in the bulk for hard sphere polymers of 20 segments. Results are shown for porosities $\epsilon = 0.085$, 0.376, and 0.922.

the increase of the bulk phase chemical potential. In other words, polymer−polymer repulsions drive more polymer into the pores. The effect is greatest when K is small, as in this case the effect of polymer−polymer repulsions in the porous material is negligible.

V. Partitioning of Polystyrene into Porous Glass

Satterfield *et al.* studied the partitioning of polystyrene into leached borosilicate glasses of various porosities.[1,28] Surface adsorption was effectively eliminated by chemically treating the glasses to remove surface hydroxyl groups. The partition coefficients were then measured using a static technique: a sample of porous material was added to a known sample of polystyrene dissolved in chloroform (a good solvent). After several

Table 1. Physical Properties of Polystyrene and Porous Glass Samples Used To Determine Model Parameters[a]

polymer sample	M_w (Da)	R_g (nm)	A_2 (cm^3 mol/g^2)	K_0 glass A	K_0 glass B	K_0 glass C
1	37 000	6.75	7.121	0.491	0.604	0.672
2	110 000	12.7	5.400	0.315	0.315	0.600
3	200 000	18.0	4.639	0.148	0.210	0.580
4	498 000	30.6	3.679		0.060	0.414
5	670 000	36.3	3.412			0.238
			porosity	0.702	0.577	0.598

days the concentration of the bulk fluid C_b was measured. A mass balance was then used to calculate the concentration in the porous material C_p.

In order to apply the semiflexible chain model to model the equilibrium properties of the polystyrene of molecular weight M_w in bulk solution and in the pores, it was necessary to determine appropriate values for certain parameters: the number of segments n, the bond length l, the segment diameter σ_p, and the stiffness parameter E. To determine n we have followed Ladd and Frenkel,[29] who assumed that each segment M_s corresponds to an atomic weight of 1000 (about 10 styrene monomers). Using a wormlike chain model, Yamakawa[30] estimated the atomic weight per unit contour length M_l to be 41.5 Å^{-1}. Enforcing the same value for our semiflexible chain, it is possible to estimate the bond length l as

$$l = \frac{M_s}{M_l} = \frac{1000}{41.5\ \text{Å}^{-1}} = 24.1\ \text{Å} = 2.41\ \text{nm} \quad (28)$$

This result may be verified by computing the constant of proportionality between the square radius of gyration and molecular weight for polystyrene at the Θ-point.

$$R_{g,\Theta}{}^2 = \frac{nl^2}{6} = \frac{1}{6}\frac{M_w}{1000}(2.41\ \text{nm})^2 = 9.68 \times 10^{-4} M_w\ \text{nm}^2 \quad (29)$$

This constant is only slightly higher than the experimental value of 8.3 × 10^{-4} nm^2 obtained by des Cloizeaux from light scattering data.[31]

To compute the diameter of the polymer segments σ_p and the stiffness parameter E, we used experimentally measured values of the second virial coefficient and the values for the radius of gyration R_g reported by Satterfield.[1] The experimentally measured second virial coefficient is usually expressed as the molar quantity A_2, which is defined by the following equation

$$\frac{\Pi}{RT} = \frac{C}{M_w} + A_2 C^2 + \ldots \quad (30)$$

where, again, Π is the osmotic pressure and C is the weight concentration of polymer, typically expressed in g/cm^3. des Cloizeaux[31] has used the results of several light scattering studies to obtain the following correlation for the second virial coefficient of polystyrene under good solvent conditions.

$$A_2 = 0.0103 M_w{}^{-0.254} \quad (\text{in units of cm}^3\ \text{mol}^{-1}\ \text{Da}^{-2}) \quad (31)$$

In statistical mechanics it is often more convenient to use the microscopic second virial coefficient B_2, defined in terms of the compressibility factor Z

$$Z = \frac{\beta\Pi}{N/V} = 1 + B_2\frac{N}{V} + \ldots = 1 + B_2\frac{\rho_p}{n} + \ldots \quad (32)$$

Equating the second terms in eqs 30 and 32 and substituting for A_2 in eq 31 yields the following expression for B_2:

$$B_2 = \frac{M_w{}^2}{N_A}A_2 = 1.7103 \times 10^{-5} M_w{}^{1.746} \quad (\text{in units of nm}^3) \quad (33)$$

B_2 can be in turn related to the activity coefficient γ by the identity

$$\left.\frac{d\ln\gamma}{d\rho_c}\right|_{\rho_c\to 0} \equiv 2\left.\frac{dZ}{d\rho_c}\right|_{\rho_c\to 0} \equiv 2B_2 \quad (34)$$

where $\rho_c = \rho_p/n$ is the number density of polymer molecules. Differentiating eq 17 and taking the limit provides the following scaled polymer expression for the second virial coefficient B_2:

$$B_2 = \frac{n^2}{2}\int_0^{\sigma_p} 4\pi\sigma_{sp}{}^2 G_{sp}(\sigma_{sp})\, d\sigma_{sp}\Big|_{\rho_p=0} \quad (35)$$

To compute the segment diameter σ_p applicable to a particular molecular weight M_w, one must first determine B_2 using eq 35 for $\sigma_p = l$ and stiffness parameter $E = 0$. A new value for σ_p can then be computed as

$$\sigma_p{}^{new} = \sigma_p\left(\frac{B_2{}^{exp}}{B_2}\right)^{1/3} \quad (36)$$

where $B_2{}^{exp}$ is the experimental value calculated from eq 33. A search technique may then be used to determine the value of E which gives the correct value for the radius of gyration R_g, shown in Table 1. The process was carried out and repeated until the relative change in σ_p was less than 0.001. The calculation usually converged in less than 10 iterations. The calculated values for σ_p and E are given in Table 2.

Table 2. Parameter Models Computed from the Physical Property Data

polymer sample	n	l (nm)	σ_p (nm)	E	σ_m(glass B) (nm)
1	37	2.41	0.955	0.298	202.9
2	110	2.41	0.911	0.575	193.5
3	200	2.41	0.880	0.738	217.1
4	498	2.41	0.824	0.988	236.1
5	670	2.41	0.809	1.065	178.7

In order to model the porous material, we used sintered, i.e., randomly placed spheres, for which $h_{mm}(r) = 0$. This model has two independent parameters: the number density of spheres ρ_m and the sphere diameters σ_m. The group $\rho_m\sigma_m{}^3$ was fixed so that the

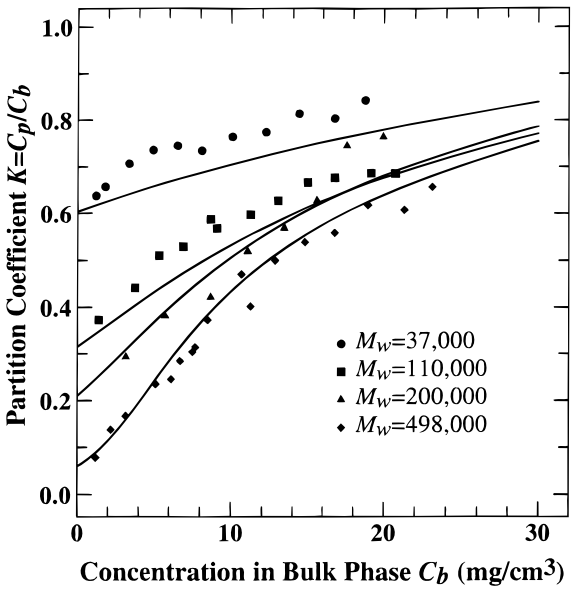

Figure 12. Partition coefficient versus bulk polymer concentration for polystyrene in a porous glass with porosity $\epsilon = 0.577$. The points are taken from the paper of Satterfield and co-workers.[1] The curves were calculated using the scaled polymer model. The arrows denote the crossover concentrations for the there largest polymers.

porosities ϵ, given eq 11, matched those reported by Satterfield and co-workers[1] using mercury porosimetry. In principle, the mercury porosimetry measurements, which also characterize the specific surface area of the material, could be applied to determine the value of σ_m. However, this approach will invariably result in an incorrect estimation of the mean pore size relevant to the polymer partitioning. We avoided this problem by using the behavior at zero concentration to determine the correct value for σ_m. By extrapolating the results of Satterfield for each combination of porous material and polymer, the zero-concentration partition coefficients or Henry's constants K_0 were estimated; these results are given in Table 1. In each case a bisection technique was used to determine the value of σ_m which produces the desired experimental value for K_0. Although this method has the undesirable feature of yielding different values of σ_m for each polymer in a single porous material, the variation is not very great, as can be seen from the values in Table 2 for glass B.

The model parameters given in Table 2 have been used to compute the K as a function of concentration for glass B. The same procedure was used as in the previous section. In order to carry out a comparison of theory and experiment, it is necessary to comment on the various definitions of K. Although the bulk phase concentration is a well-defined quantity, the concentration in the pore phase is not unique because of the uncertain value of the volume occupied by the fluid in a heterogeneous environment. In experimental studies such as that of Satterfield *et al.*[1] that volume is normally calculated from measurements of the porosity ϵ. In statistical mechanics it is more convenient to consider instead the entire volume occupied by both the fluid and porous material.[32,33] In our discussions we have used the latter definition, $K \equiv \rho_p/\rho_p^b$, where the superscript b refers to the bulk fluid (where $\rho_m = 0$). The corresponding experimental definition for the partition coefficient is simply $K_{exp} \equiv \rho_p/\epsilon\rho_p^b$.

The results for four different polymer samples are shown in Figure 12, along with the original experimental data. At low concentration, the agreement is good, by construction. Additionally, the model accurately predicts the way in which K increases with concentration. The model is seen to be best for the larger molecules, where the concentration effect is more pronounced. This may be a result of specific polymer−substrate attractive interactions, which are probably more important for smaller molecules. Molecule−molecule interactions within the pores are also more important for the smaller molecules.

VI. Summary

Our calculations illustrate the application of an integral equation model to the calculation of the thermodynamic properties of polymer solutions in random porous materials. A new equation relating structural properties to thermodynamic properties has been developed. This scaled polymer equation provides very accurate equation of state predictions for hard sphere chain fluids in the bulk and gives much better agreement with simulation than previously developed equations based on integral equation theory. The scaled polymer method also accurately predicts the partitioning of hard sphere chains from an infinitely dilute solution into a packed bed of quenched hard spheres. We have also found that the concentration effect on partitioning is driven by deviations from ideality, first it the bulk solution and then in the pore solution. The effect is greatest when the zero-concentration partition coefficient K_0 is small. We have used the scaled polymer approach to model experimental results for the partitioning of polystyrene in a good solvent into porous glasses. Good agreement is achieved for the larger molecular weights. The theory underpredicts the concentration effect for the smaller molecules.

Acknowledgment. The authors acknowledge the support of the U.S. Department of Energy, Office of Basic Energy Sciences. They are also grateful to David M. Ford for useful discussions.

References and Notes

(1) Satterfield, C. N.; Colton, C. K.; Turckheim, B.; Copeland, T. M. Effect of Concentration on Partitioning of Polystyrene within Finely Porous Glass. *AIChE J.* **1978**, *24*, 937.

(2) Brannon, J. H.; Anderson, J. L. Concentration Effects of Partitioning of Dextrans and Serum Albumin in Porous Glass. *J. Polym. Sci., Polym. Phys. Ed.* **1982**, *20*, 857.

(3) Yethiraj, A.; Hall, C. K. Integral Equation Theory for the Adsorption of Chain Fluids in Slitlike Pores. *J. Chem. Phys.* **1991**, *95*, 3749.

(4) Bleha, T.; Cifra, P.; Karasz, F. E. The Effects of Concentration on Partitioning of Flexible Chains into Pores. *Polymer* **1990**, *31*, 1321.

(5) Bleha, T.; Spychaj, T.; Vondra, R.; Berek, D. Concentration Effects and Thermodynamic Non-ideality in Gel Chromatography. *J. Polym. Sci., Polym. Phys. Ed.* **1983**, *21*, 1903.

(6) Teraoka, I.; Langley, K. H.; Karasz, F. E. Diffusion of Polystyrene in Controlled Pore Glasses: Transition from the Dilute to the Semidilute Regime. *Macromolecules* **1993**, *26*, 287.

(7) Thompson, A. P.; Glandt, E. D. Adsorption of Polymeric Fluids in Microporous Materials. I. Ideal Freely Jointed Chains. *J. Chem. Phys.* **1993**, *99*, 8325.

(8) Chandler, D. RISM Equations for Fluids in Quenched Amorphous Materials. *J. Phys. Condensed Matter* **1991**, *42*, F1.

(9) Schweizer, K. S.; Curro, J. G. Integral Equation Theory of Polymer Melts: Intramolecular Structure, Local Order, and the Correlation Hole. *Macromolecules* **1988**, *21*, 3070.

(10) Madden, W. G.; Glandt, E. D. Distribution Functions for Fluids in Random Media. *J. Stat. Phys.* **1988**, *51*, 537.

(11) Madden, W. G. Fluid Distribution in Two Phase Random Media: Arbitrary Matrices. *J. Chem. Phys.* **1992**, *96*, 5422.
(12) Ford, D. M.; Thompson, A. P.; Glandt, E. D. Thermodynamics of Fluids in Random Microporous Materials from Scaled Particle Theory. *J. Chem. Phys.*, submitted.
(13) Gao, J.; Weiner, J. H. Contribution of Covalent Bond Force to Pressure in Polymer Melts. *J. Chem. Phys.* **1989**, *91*, 3168.
(14) Chandler, D.; Andersen, H. C. Optimized Cluster Expansions for Clasical Fluids II: Theory of Molecular Liquids. *J. Chem. Phys.* **1972**, *57*, 1930.
(15) Hansen, J. P.; McDonald, I. R. *Theory of Simple Liquids*; Academic: London, 1986.
(16) Honnell, K. G.; Curro, J. G.; Schweizer, K. S. Local Structure of Semiflexible Polymer Melts. *Macromolecules* **1990**, *23*, 3496.
(17) Verlet, L.; Levesque, D. *Physica* **1967**, *36*, 254.
(18) Lowden, L. J.; Chandler, D. Solution of a New Integral Equation for a Pair of Correlation Functions in Molecular Liquids. *J. Chem. Phys.* **1973**, *59*, 6587. Chandler, D. In *Studies in Statistical Mechanics VIII;* E. W., Montroll, J. L., Lebowitz, Eds.; North-Holland: Amsterdam, 1982.
(19) Schweizer, K. S.; Curro, J. G. Integral Equation Theory of the Structure of Polymer Melts. *Phys. Rev. Lett.* **1987**, *58*, 246.
(20) Hill, T. L. *Statistical Mechanics*; McGraw-Hill: New York, 1956.
(21) Schweizer, K. S.; Curro, J. G. Equation of State of Polymer Melts: Formulation. *J. Chem. Phys.* **1988**, *89*, 3342.
(22) Schweizer, K. S.; Curro, J. G. Equation of State of Polymer Melts: Results. *J. Chem. Phys.* **1988**, *89*, 3350.
(23) Reiss, H.; Frisch, H. L.; Lebowitz, J. L. *J. Chem. Phys.* **1959**, *31*, 369. Lebowitz, J. L.; Helfand, E.; Praestgaard, E. *J. Chem. Phys.* **1965**, *43*, 774.
(24) Ford, D. M.; Glandt, E. D. Compressibility Equation for Fluids in Random Microporous Matrices. *J. Chem. Phys.* **1994**, *100*, 2391.
(25) Dickman, R.; Hall, C. K. Equation of State for Chain Molecules: Continuous-Space Analog of Flory Theory. *J. Chem. Phys.* **1986**, *85*, 4108.
(26) Frenkel, D.; Smit, B. Unexpected Length Dependence of the Solubility of Chain Molecules. *Mol. Phys.* **1992**, *75*, 983.
(27) Reid, T. M.; Gubbins, K. E. *Applied Statistical Mechanics*; McGraw-Hill: New York, 1973.
(28) Colton, C. K.; Satterfield, C. N.; Lai, C. J. Diffusion and Partitioning of Macromolecules within Finely Porous Glass. *AIChE J.* **1975**, *21*.
(29) Ladd, A. J. C.; Frenkel, D. Computer Simulation Studies of Static and Dynamic Scaling in Dilute Solutions of Excluded Volume Polymers. *Macromolecules* **1992**, *25*, 3435.
(30) Yamakawa, H. *Modern Theory of Polymer Solutions*; Harper and Row: New York, 1971.
(31) des Cloizeaux, J.; Jannink, G. *Polymers in Solution: Their Modelling and Structure*; Clarendon Press: Oxford, 1990.
(32) Glandt, E. D. Distribution Equation between a Bulk Phase and Small Pores. *AIChE J.* **1981**, *27*, 51.
(33) Anderson, J. L.; Brannon, J. H. Concentration Dependence of the Distribution Coefficient for Macromolecules in Porous Media. *J. Polym. Sci., Polym. Phys. Ed.* **1981**, *19*, 405.

MA9503219